Analysis of the fluorescence signal from a single droplet using a model based on the Lorenz Mie Theory and on ray tracing methods

B. Frackowiak* and C. Tropea
Institute for Fluid Mechanics and Aerodynamics, Technische Universität Darmstadt,
Petersenstr. 30, 64287 Darmstadt, Germany

Abstract

Laser Induced Fluorescence (LIF) has been previously used in various forms to characterize droplets in a spray, according to either size or temperature. An examination of the LIF signal is performed with a fluorescence model based on the Generalized Lorenz Mie Theory (GLMT) and on ray-tracing methods, for n-heptane droplets seeded by 3-pentanone uniformly illuminated by a laser beam, and for a water droplet seeded by Rhodamine 6G and passing through one or two highly focussed laser beams. In the first case, a parametric study quantifies the bias caused not only by the absorption of the laser, but also by shadow zones in the droplets which do not contribute to the fluorescence signal. In the second case, the time-of-flight measurements suggest several avenues for using LIF scattering for size and velocity measurements of individual droplets.

Introduction

Laser Induced Fluorescence (LIF) is commonly applied in two-phase flow diagnostics, relying on the excitation of fluorescing molecules at a specific wavelength [1, 2, 3, 4, 5, 6, 7, 8, 9, 10, 11, 12], and on the conversion of the fluorescence signal into a voltage using an appropriate detector, or into an image using an intensified camera, possibly with bandwidth filters. In the Planar Droplet Sizing (PDS), the image corresponding to the plane of a laser sheet illuminating the spray is acquired by an intensified CCD camera. The combination of the fluorescence with the Mie scattering provides ideally the Sauter Mean Diameter (SMD) of the spray [13, 14, 15, 16], assuming that the amplitude of the fluorescence scattering depends on the droplet volume and the amplitude of the Mie scattering on the droplet surface area. Nevertheless, a bias is induced in the fluorescence scattering, caused either by the absorption of the laser fluence by the dye, or by the focusing of the laser or fluorescence rays when they traverse the interface entering or leaving the droplet.

Previous investigations of this issue have been carried out at a fundamental level by Domann et al.[15], using a water droplet seeded by Rhodamine 6G, at concentrations ranging between $0.001\,g.L^{-1}$ and $0.1\,g.L^{-1}$. A purely empirical correlation between the diameter d and the fluorescence signal $S_{fluo,droplet}$ has been suggested, relying on a constant $\mathcal{K}_f$ and on an exponent b_f, ranging from 3 for a fluorescence dependence on the droplet volume to 2 for a dependence on the droplet surface area.

$$S_{fluo,droplet} = \mathcal{K}_f \times d^{b_f} \tag{1}$$

A more thorough investigation of the fluorescence signal illuminated by one or several laser beams is proposed in the present study by applying a fluorescence model [1] on a single n-heptane droplet seeded with 3-pentanone illuminated by a uniform monochromatic UV laser beam at $266\,nm$ and on a water droplet seeded by Rhodamine 6G and passing through one or two highly focussed laser beams. A parametric study is carried out in order to quantify the effect of the absorption in the liquid phase and of the focussing of the laser or fluorescence rays at the liquid-gas interface. Moreover, the time-of flight fluorescence signal obtained with droplets when they traverse the focussed laser beams is examined, as a function of droplet diameter and trajectory.

Materials and Methods

The calculations are performed with a fluorescence model [1] based on the Generalized Lorenz Mie Theory (GLMT) [18, 19] and on ray-tracing methods, assuming that the droplet is spherical. The GLMT theory provides either the axisymmetric fluence field E_{liq} inside the droplet considering the laser as a monochromatic plane wave and neglecting the polarisation or the 3D fluence field obtained with the focused beams. In each case, the laser beam is aligned with the x axis. The liquid is assumed to be a homogeneous mixture, with absorption taken into

*Corresponding author: bruno.frackowiak@sla.tu-darmstadt.de

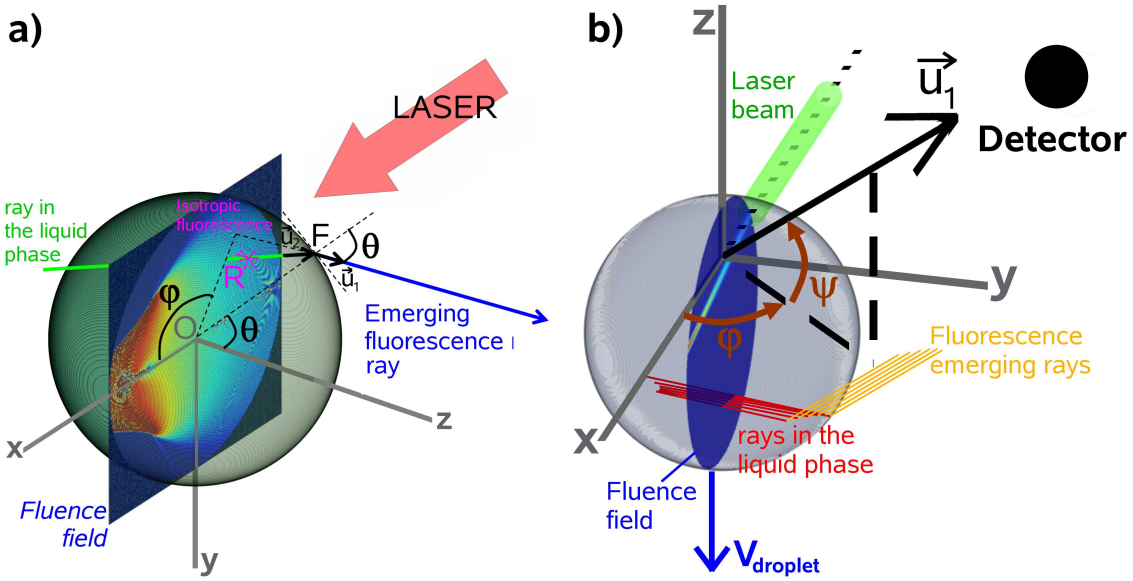

Figure 1. Geometric arrangement of laser, droplet and detector. a) PDS b) focussed laser beams

account through the imaginary part of the refractive index $n_{i,droplet}$. For the droplets traversing the focussed laser beam, the mixture is transparent.

In the ray tracing method (Fig. 1), the emerging fluorescence rays are computed from the droplet surface: one angular direction $\vec{u_1}$ is considered, assuming a small aperture of the photodetector or the camera in comparison with its distance from the measurement zone; i.e. a point detector. This direction $\vec{u_1}$ is orientated perpendicularly to the laser beam for the PDS, and according to two angles Ψ and φ for the droplets traversing the focussed laser beam. The Snell-Descartes law combined with the optical reciprocity principle yields the direction inside the droplet of each fluorescence ray emerging from the surface. The fluorescence value of each ray is determined by integrating the local fluorescence S_{fluo} along the ray (Eq. 2), which is assumed to be isotropic and proportional to the local fluence, taking into account the transmission factor T_{fluo} at the droplet surface. This yields a volume integral equation. Nevertheless, it can be discretized according to a line integral, by considering the fixed area of one pixel inherent to the image resolution. Otherwise, the internal reflections of the fluorescence rays are neglected.

$$S_{fluo,ray} = T_{fluo} \times \int_{ray} S_{fluo}\, dV = T_{fluo} \propto \int_{ray} E_{liq}\, dV \tag{2}$$

The focusing of the laser rays can be disabled for the fluence field by using a simpler model based on the Beer Lambert absorption. This model effectively assumes that the laser rays are not deflected when they traverse the interface into the droplet, and propagate solely in the $\vec{e_x}$ direction inside the droplet. Moreover, the focusing of the fluorescence rays is also investigated, by comparing the complete ray tracing method using the correct real part of the refractive index $n_{droplet}$ and a simplified method using a value equal to 1 to disable the deflection of the rays.

Results and Discussion

Fluorescence for the PDS

First results of the fluence field in the droplet and fluorecence images at the camera are shown in Fig. 2 for various droplet sizes and absorption levels. From these results it is clear that there are two significant effects determining the final fluorescence image:

- the focussing of the laser rays towards the half side of the droplet opposite to the laser side, dominating when the droplet is small with a weak absorption coefficient
- the Beer-Lambert absorption of the laser rays, dominating when the droplet is large, with a strong absorption coefficient

A parametrical study is carried out, considering the empirical correlation (Eq. 1) between the diameter d and the fluorescence signal of the droplet $S_{fluo,droplet}$. Four different cases are pictorially shown in Fig. 3a:

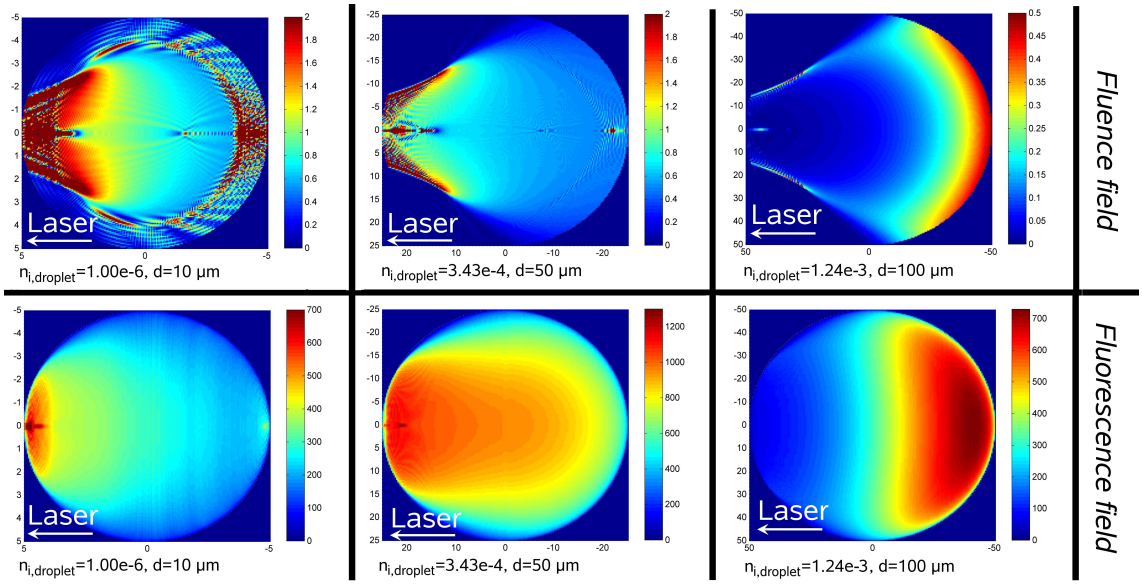

Figure 2. Fluence field inside the droplet and fluorescence images at the camera for various droplet sizes and absorption levels. Note the large variation of colour scales.

- the complete LMT computation combined with the complete ray-tracing method
- only the Beer-Lambert fluence field combined with the complete ray-tracing method
- the complete LMT computation without focussing of the fluorescence rays ($n_{droplet} = 1$)
- only the Beer-Lambert fluence field without focussing of the fluorescence rays ($n_{droplet} = 1$)

The variation of the b_f exponent versus $n_{i,droplet}$ (Fig. 3b) exhibits a fluorescence dependence on the volume ($b_f = 3$) for low absorbing mixtures and a fluorescence dependence on the surface area ($b_f = 2$) for highly absorbing mixtures. In-between, two different behaviours are observed. When the focussing of the fluorescence rays is disabled ($n_{droplet} = 1$), b_f presents a monotonic decrease from 3 to 2, whereas when the focussing of the fluorescence rays is enabled, b_f decreases below values of 2 and then increases again. For both cases, the computation of the fluence field with the complete GLMT or with the Beer-Lambert law results in a slight horizontal shift between the respective curves, without affecting their shape.

A further analysis carried out with the fluorescence signal plotted versus $n_{i,droplet}$ for a $100\,\mu m$ droplet (Fig. 3c) confirms also these two different behaviours. When the focussing of the fluorescence rays is disabled ($n_{droplet} = 1$), the fluorescence signal increases continuously with absorption coefficient and reaches an asymptotic value, whereas a sharp maximum is observed when the focussing of the fluorescence rays is enabled, followed by a decrease to a lower asymptotic value. In both cases, for highly aborbing mixtures, the computation of the fluence field with the complete LMT or with the Beer-Lambert law results in the same respective asymptotic values, because the fields becomes identical without any effect of the focussing of the laser rays.

The focussing of the fluorescence rays evidently results in shadow zones inside the droplet close to the surface, where the fluorescing molecules do not contribute to the fluorescence signal even if they are illuminated by the laser. The fluorescent molecules located close to the focal point contribute much stronger to the fluorescence signal. This justifies the lower asymptotic fluorescence value obtained with highly absorbing mixtures, whereas the maximum of fluorescence is obtained for intermediate mixtures, where the concentration is sufficiently strong to provide a quantum yield, but sufficiently low to allow a significant illumination of the molecules located close to the focal point of the fluorescence rays.

Regarding fuel spray diagnostics, the focussing of the fluorescence rays modifies the shape of the curve and the values of the exponents b_f (Fig. 3b): the fluorescence dependence on the surface area ($b_f = 2$) is reached for the pure 3-pentanone and the decrease remains significant with the focussing, whereas the b_f values are higher without the focussing, yielding a curve with a more rounded shape. Otherwise, good agreement is obtained with the results of Domann et al.[15] for concentrations ranging between $0.001\,g.L^{-1}$ and $0.1\,g.L^{-1}$ i.e. for $n_{i,droplet}$ ranging between $1e^{-6}$ and $1e^{-4}$ (Table 1). This last comparison is valid because of the negligible difference between the real parts of the refractive index for water and n-heptane.

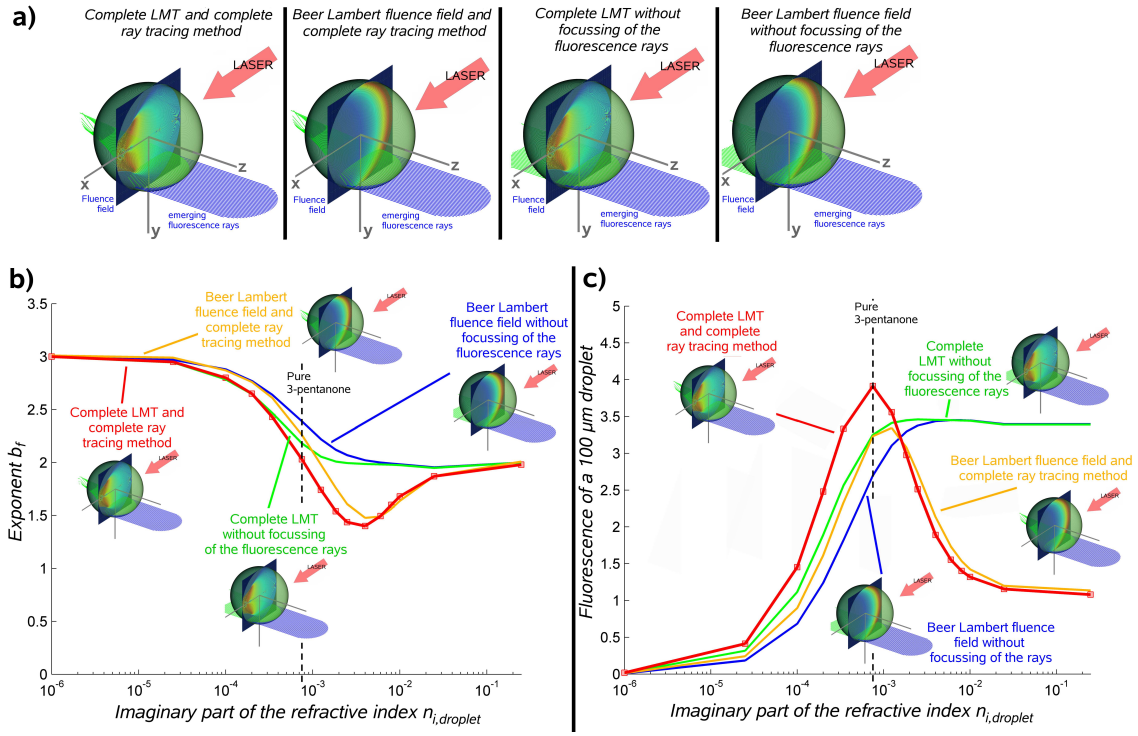

Figure 3. a) Different cases considered for the quantitative evaluation of overall fluorescence intensity. b) and c) Variation of the b_f exponent and of the fluorescence signal ($100\,\mu m$ droplet) versus $n_{i,droplet}$

Fluorescence with the focussed laser beams

Different detector positions are now considered using a $100\,\mu m$ droplet (Fig. 4a)), either in the xy plane ($\Psi = 0\,^\circ$) or in the the yz plane ($\varphi = 90\,^\circ$). Non-symmetric profiles are obtained with the detector positioned in the yz plane ($\varphi = 90\,^\circ$), when Ψ is different from 0°. Indeed, when Ψ is equal to $+45^\circ$, the focussing of the fluorescence rays leads to a stronger contribution of the liquid on the lower side of the droplet, which is illuminated by the beam when $z_{droplet}$ is positive and leads to a higher fluorescent signal. For the opposite case of Ψ equal to -45°, the fluorescence values are higher when $z_{droplet}$ is negative. Profiles obtained with the detector positioned in the xy plane ($\Psi = 0\,^\circ$) exhibit symmetric shapes with different amplitudes and sharp maxima when the detector orientation corresponds to the laser beam plane ($\varphi = 0\,^\circ$ or $\varphi = 180\,^\circ$).

In a real measurement system, the angle Ψ can be estimated by comparing both sides of one profile, whereas the angle φ can be deduced by comparing the amplitude of the profiles obtained with different detectors. Otherwise, the droplet diameter can be determined from the width of the signal profile, because no time shift is observed in the fluorescence signal whatever the detection angle (Fig. 4a)) and the width increases linearly with this diameter (Fig. 4b)). For the conversion of signal width (duration) to a spatial distance, a velocity measurement would be required, which would be possible by using a two beam arrangement and a time-of-flight measurement. In practice, laser sheets rather than focussed beams could reduce the trajectory dependence of the signal, as has been demonstrated for the time-shift technique of particle sizing and velocity measurement [17]. Alternatively the LIF system could be combined with a laser Doppler system, as demonstrated in [8].

Conclusion

A fluorescence model has been successfully applied to a single droplet. The bias in the PDS method in measuring SMD has been precisely quantified, emphasizing the effect of the liquid absorption and of the focussing of the rays when they traverse the interface. Moreover, the time-of-flight measurement of the fluorescence signal profile with high focused laser beams can be used to measure not only the droplet diameter from the profile width, but also the trajectory direction and velocity. The use of a laser sheet or an overlayed laser Doppler system may be advantageous to improve the accuracy of these velocity measurements.

Table 1. Imaginary part of the refrative index $n_{i,droplet}$ for various mixtures from Domann et al.[15] and from the present study

Rhodamine seeded in water	$0.001\,g.L^{-1}$	$0.01\,g.L^{-1}$	$0.001\,g.L^{-1}$
	$n_{i,droplet} = 1e^{-6}$	$n_{i,droplet} = 1e^{-5}$	$n_{i,droplet} = 1e^{-4}$
	$b_f = 2.99$	$b_f = 2.95$	$b_f = 2.75$
3-pentanone mixed in nheptane	$15\,\%$	$30\,\%$	$100\,\%$
	$n_{i,droplet} = 1e^{-4}$	$n_{i,droplet} = 2e^{-4}$	$n_{i,droplet} = 7.5e^{-4}$
	$b_f = 2.792$	$b_f = 2.645$	$b_f = 2.027$

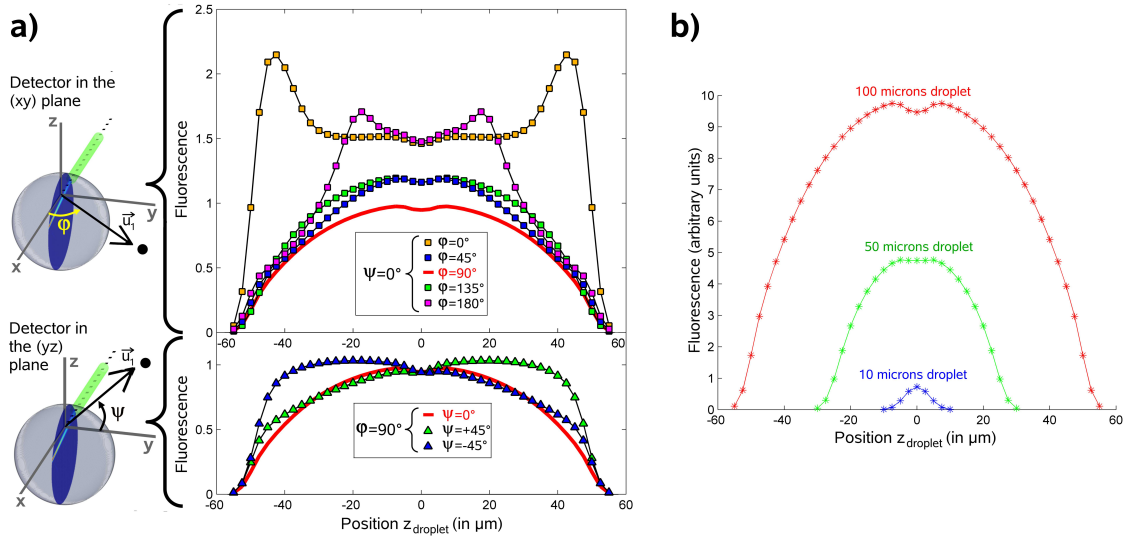

Figure 4. Time-of-flight measurement of the fluorescence of a droplet traversing a focussed laser beam. a) Influence of the detector position. b) Influence of the droplet diameter

Aknowledgements

This work has been supported by the Deutsche Forschungsgemeinschaft (GRK 1114). The authors aknowledge also the CORIA laboratory [18, 19], who developed the LMT software to compute the 3D fluence fields in the droplet.

References

[1] B. Frackowiak, A. Strzelecki, G. Lavergne, "A liquid-vapor interface positioning method applied to PLIF measurements around evaporating monodisperse droplet streams", *Experiment in Fluids* 46:671-682 (2009)

[2] Schulz C., Sick V. "Tracer-LIF diagnostics: Quantitative measurement of fuel concentration, temperature and air/fuel ratio in practical combustion situations" *Prog. Energy Combust. Sci.* 31:75-121 (2005)

[3] Thurber M. C. "Acetone Laser Induced Fluorescence for temperature and multiparameter imaging in gaseous flows". Thesis report TSD-120, Stanford University (1999)

[4] Thurber M. C., Grisch F., Kirby B. J., Vostmeier M., Hansom R. K. "Measurements and modelling of acetone Laser Induced Fluorescence with implication for temperature imaging diagnostics" *Applied Optics* 37:4963-

4978 (1998)

[5] Castanet G., Lavieille P., Lebouché M., Lemoine F., "Measurement of the temperature distribution within monodisperse combusting droplets in linear streams using two-color laser-induced fluorescence", *Exp. in Fluids* 35:563-571 (2003)

[6] Castanet G., Delconte A., Lemoine F., "Evaluation of the temperature gradients within combusting droplets in linear stream using two colors laser-induced fluorescence", *Exp. in Fluids* 39:431-440 (2005)

[7] Castanet G., Lebouché M., Lemoine F., "Heat and mass transfer of combusting monodisperse droplets in a linear stream", *Int. J. Heat and Mass Transfer* 48:3261-3275 (2005)

[8] Maqua C., Castanet G., Doué N., Lavergne G., Lemoine F., "Temperature measurements of binary droplets using three colors induced fluorescence", *Exp. in Fluids* 40:786-797 (2006)

[9] Lavieille P., Lemoine F., Lavergne G., Virepinte J.F., Lebouché M. "Temperature measurements on droplets in monodisperse stream using laser induced fluorescence", *Exp. in Fluids* 29:429-437 (2000)

[10] Lavieille P., Lemoine F., Lavergne G., Lebouché M. "Evaporating and combusting droplet temperature measurements using two-color laser induced fluorescence", *Exp. in Fluids* 31:45-55 (2001)

[11] Lavieille P., Lemoine F., Lebouché M. "Investigation on temperature of evaporating droplet in linear stream using two-color laser induced fluorescence", *Combustion Science and Technology* 174:117-142 (2002)

[12] Lavieille P., Delconte A., Blondel D., Lebouché M., Lemoine F. "Non-intrusive temperature measurements using three-color laser-induced fluorescence", *Exp. in Fluids* 36:706-716 (2004)

[13] Domann R., Hardalupas Y., "Spatial distribution of fluorescence intensity within large droplets and its dependence on dye concentration", *Applied Optics* 40:3586-3597 (2001)

[14] Domann R., Hardalupas Y., "A study of Parameters that influence the Accuracy of the Planar Droplet Sizing (PDS) Technique", *Part. Part. Syst. Charact.* 18:3-11 (2001)

[15] Domann R., Hardalupas Y., Jones A. R., "A study of the influence of absorption on the spatial distribution of fluorescence intensity within large droplets using Mie theory, geometrical optics and imaging experiments", *Measurement Science and Technology* 13:280-291 (2002)

[16] Domann R., Hardalupas Y., "Quantitative Measurement of Planar Droplet Sauter Mean Diameter in Sprays using Planar Droplet Sizing", *Part. Part. Syst. Charact.* 20:209-218 (2003)

[17] Damaschke N., Nobach H., Semidetnov N., Tropea C., "Optical particle sizing in backscatter", *Applied Optics* 41:5713-5727 (2002)

[18] Méès L., Gouesbet G., Gréhan G., "Interactions between femtosecond pulses and a spherical microcavity: internal fields", *Opt. Commun.* 199:33-38 (2001)

[19] Li R., Han X., Shi L., Ren K. F., Jiang H., "Debye series for Gaussian beam scattering by a multilayered sphere", *Applied Optics* 46:4804-4812 (2007)